ACS OMEGA

Article

Cite This: ACS Omega 2018, 3, 8760−8768

http://pubs.acs.org/journal/acsodf

α,ε-Hybrid Peptide Foldamers: Self-Assembly of Peptide with Trans Carbon−Carbon Double Bonds in the Backbone and Its Saturated Analogue

Mintu Debnath, Tanmay Das, Debasish Podder, and Debasish Haldar*

Department of Chemical Sciences, Indian Institute of Science Education and Research Kolkata, Mohanpur 741246, West Bengal, India

Supporting Information

ABSTRACT: The effect of geometrically rigid trans α,β-unsaturated ε-amino acids on the structure, folding, and assembly of α,ε-hybrid peptide foldamers has been reported. From single-crystal diffraction analysis, the unsaturated tetrapeptide **1** has stapler-pin-like structure but without intramolecular hydrogen bond. The asymmetric unit has two molecules that are stabilized by multiple intermolecular hydrogen bonding interactions as well as π−π stacking interactions between the aromatic rings of 3-amino-cinnamic acid. Peptide **1** does not form organogel. But on hydrogenation, peptide **1** provides the saturated α,ε-hybrid peptide foldamer **2**, which forms instant gel in most of the aromatic solvents. The gel exhibits high stability. The unsaturated peptide **1** has porous microsphere morphology, but saturated analogue **2** has ribbonlike morphology. The gel has been used efficiently for removal of cationic organic pollutants from waste water.

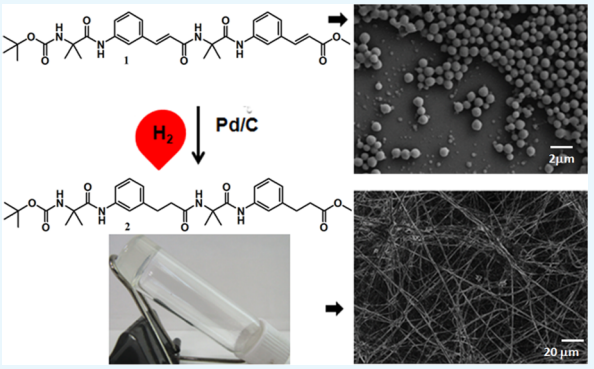

INTRODUCTION

To mimic the structure and function of well-folded biopolymers, like peptides, proteins, and DNA, synthetic oligomers containing designer building blocks that exhibit distinct conformational characteristics have promoted many recent advances in foldamers' study.[1−3] The incorporation of noncoded β-, γ-, δ-, or ε-amino acids into folded structures with α-amino acid chains has been widely used in the design of foldamers having hybrid backbones.[4−6] Previously, foldamer studies mainly focused on design and synthesis of new secondary motifs, a goal that is still alive, but recent trends have expanded to include functionality in foldamers.[7−10] Introducing a conformational bias by incorporating conformationally rigid amino acid residues has been shown to increase the crystallinity of foldamers.[11] This is reported by substantial solid state studies of peptides containing α-aminoisobutyric acid (Aib) or allied α,α-dialkylated amino acid residues.[12,13] But the crystallographic analysis of hydrogen-bonded novel hybrid peptides has been possible in peptides containing stereochemically constrained unsaturated amino acids, where the auxiliary degrees of backbone torsional rotation have been restricted by unsaturation.[14−16] For example, Gopi and co-workers have reported the unsaturated amino acid-triggered folding of polypeptides.[17] But controlling molecular orientation and diverse degrees of self-assembly of unsaturated peptides in comparison to controlling those of their saturated analogues is still challenging.[18]

Herein, we have synthesized a tetrapeptide containing trans α,β-unsaturated ε-amino acid and α-aminoisobutyric acid. Although the 3-(3-aminophenyl)propionic acid has been extensively investigated in biology and material science,[19,20] very little is known about the conformational properties of the unsaturated analogue 3-aminocinnamic acid. The natural existence and very good bioactivities of unsaturated amino acids motivated us to examine the conformational preferences of these amino acids in hybrid peptides. Aib is helicogenic and conformationally rigid. 3-Aminocinnamic acid is also geometrically constrained. So introduction of Aib and 3-amino-cinnamic acid will be fascinating not only for molecular structure but also for directing molecular orientation (for adjustment of steric factors) and crystal packing (Figure 1). Interestingly, the α,ε-hybrid peptide **1** exhibits stapler-pin-like conformation in solid state. The two peptide molecules in the asymmetric unit are antiparallel and stabilized by multiple intermolecular hydrogen bonding interactions and π−π stacking interactions. Hybrid peptide **1** does not form gel in organic solvents. However, on hydrogenation, peptide **1** provides saturated analogue α,ε-hybrid peptide **2**, which forms instant gel in most of the aromatic solvents. Field emission scanning electron microscopy (FE-SEM) reveals that peptide **1** has porous microsphere morphology but peptide **2**

Received: April 27, 2018
Accepted: July 24, 2018
Published: August 8, 2018

DOI: 10.1021/acsomega.8b00832
ACS Omega 2018, 3, 8760−8768

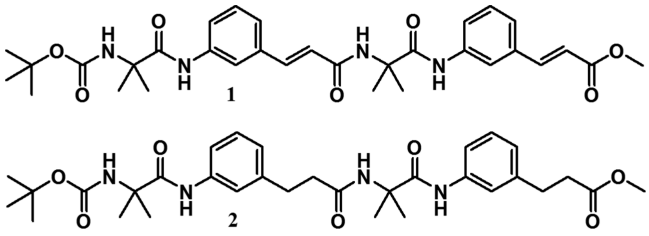

Figure 1. Chemical structures of α,ε-hybrid peptides **1** and **2**.

has ribbons-like morphology. Moreover, the organogel of α,ε-hybrid peptide **2** is used efficiently to remove organic pollutants from waste water.

RESULTS AND DISCUSSION

The noncoded amino acid trans-3-aminocinnamic acid methyl ester was synthesized by the condensation reaction between 3-nitrobenzaldehyde and malonic acid in dimethylformamide−water medium at 120 °C for 6 h, followed by esterification with thionyl chloride in methanol at room temperature and finally the reduction of the nitro group with iron−acetic acid at 100 °C for 3 h (Scheme 1).

Scheme 1. Synthesis of Methyl (*E*)-3-Aminocinnamate 6

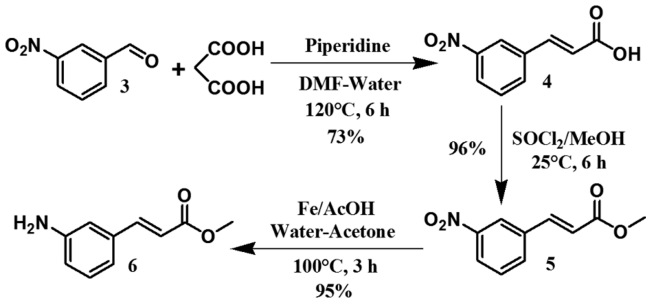

The α,ε-hybrid peptide foldamer **1** was synthesized using traditional solution-phase peptide coupling methodology by dicyclohexylcarbodiimide (DCC) as a coupling reagent (Figure 2). Foldamer **2** has been synthesized by reduction of foldamer **1** with hydrogen and Pd/C catalyst in methanol (Figure 2). The disappearance of characteristic cinnamic acid signals and appearance of new signals for 3-phenylpropanoic acids in the ^{1}H NMR spectrum indicates the formation of peptide **2** from peptide **1**. The synthesized compounds and intermediates were purified by column chromatography and analyzed by ^{1}H NMR, ^{13}C NMR, Fourier transform infrared (FT-IR), and mass spectrometry.

First, we have investigated the assembly of α,ε-hybrid peptide foldamers **1** and **2** in solution using different spectroscopic experiments. The solution state UV/vis spectra shows no change of spectral positions (249 and 278 nm for $\pi-\pi^*$ transition), but intensity of absorption increases with increasing peptide **1** concentration in methanol (Figure 3a). For peptide **2**, the typical absorption band in methanol solution at 244 nm increases with increasing peptide concentration (Figure 3b). The results suggest that irrespective of unsaturation and rigidity, the intermolecular interactions for both the peptides are similar.

FT-IR spectroscopy is a superb experiment to investigate the structure and self-assembly patterns of peptides. The unsaturated α,ε-hybrid peptide **1** exhibits N−H stretching

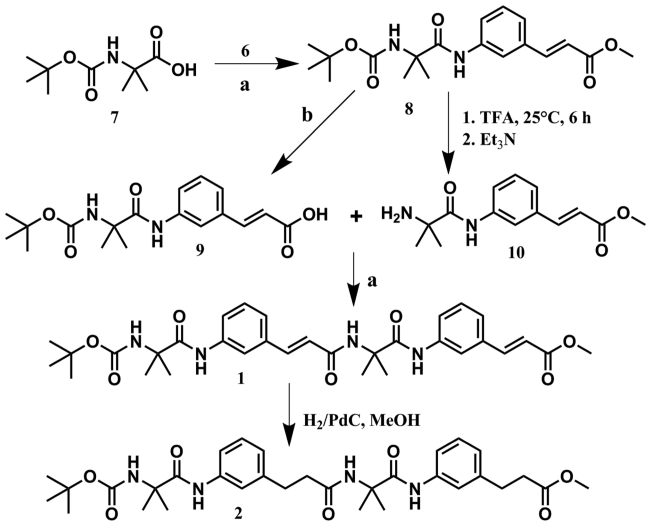

Figure 2. Reactions and conditions: (a) DCC, dry dichloromethane (DCM), 273 K, Et_3N, 48 h, 48−58% (b) 1 N NaOH, MeOH, 300 K, 12 h, HCl, 83%.

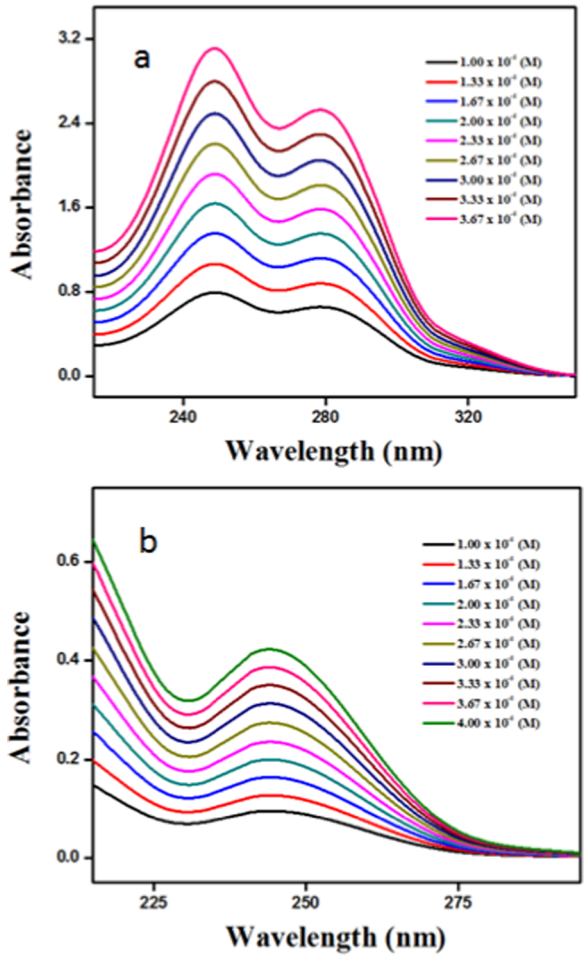

Figure 3. UV/vis spectra of (a) peptide **1** and (b) peptide **2** with increasing concentration in methanol.

vibrations at 3365 cm^{-1} and amide I and amide II exhibit peaks at 1677 and 1535 cm^{-1}, respectively.[21] However, the saturated α,ε-hybrid peptide **2** shows N−H stretching vibration at 3430 cm^{-1} and amide I and amide II show peaks at 1651 and 1584

DOI: 10.1021/acsomega.8b00832
ACS Omega 2018, 3, 8760−8768

cm^{-1}, respectively (Figure 4).[21] Hence, the peptide backbone changes on hydrogenation.

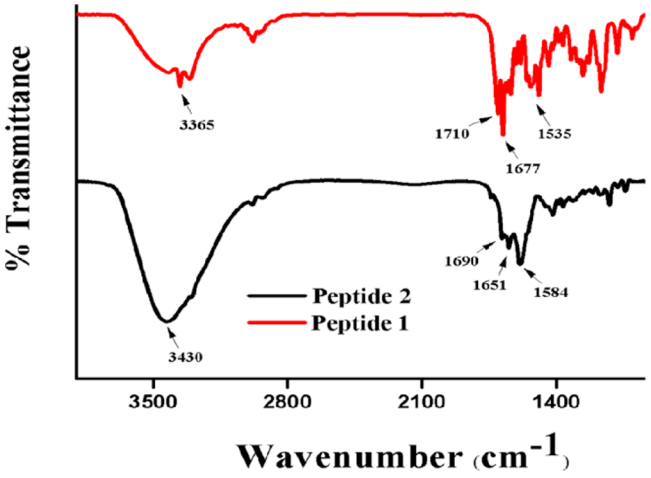

Figure 4. FT-IR spectra of peptides **1** and peptide **2**.

To explore the molecular conformation and self-assembly pattern of the 3-aminocinnamic acid containing α,ε-hybrid peptide foldamer **1**, single-crystal X-ray crystallography was performed. Light yellow color monoclinic crystals of peptide **1** were obtained from methanol−water solution by slow evaporation. There are two molecules of peptide **1** in the asymmetric unit (Figure 5) in antiparallel arrangement.[22] The

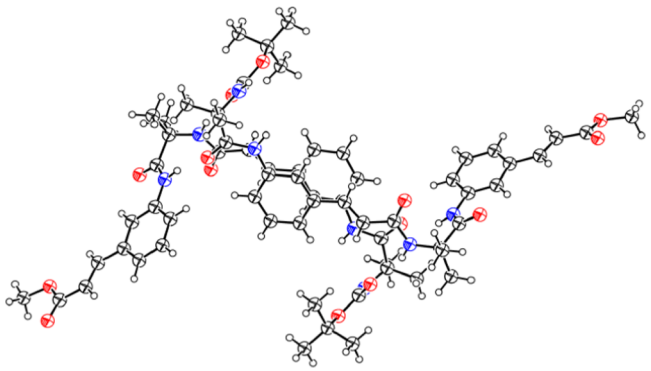

Figure 5. Oak Ridge thermal ellipsoid plot diagram of α,ε-hybrid peptide foldamer **1** showing antiparallel arrangement of molecules (50% probability).

two molecules are stabilized by four intermolecular N−H···O hydrogen bonds between Aib NH and Boc C═O and 3-aminocinnamic acid NH and Aib C═O. A strong face to face $\pi-\pi$ stacking interaction between 3-aminocinnamic acid moieties stabilized the dimer. The centroid to centroid distance is 3.621 Å (Figure 6). The α,ε-hybrid peptide foldamer **1** adopts stapler-pin-like conformation in solid state. The ϕ and ψ values of the Aib residues are in the helical region of the Ramachandran diagram. Table 1 shows the important backbone torsion angles of peptide **1**. In higher order packing, the peptide **1** molecules self-assemble to form a porous structure (Figure 7) through intermolecular hydrogen bonding and $\pi-\pi$ stacking interactions. The diameters of the pores are 4.4 and 6.1 Å. Table 2 shows the hydrogen bonding parameters of peptide **1**. We have tried to crystallize peptide **2** from different solutions but failed to obtain X-ray quality crystal.

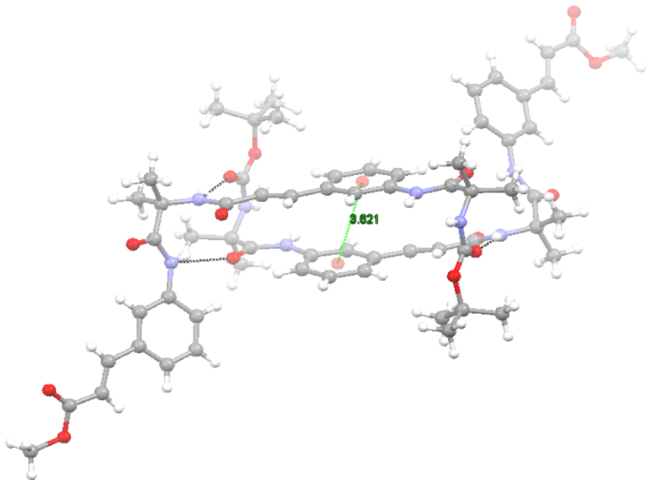

Figure 6. Dimer showing face to face $\pi-\pi$ stacking. Intermolecular hydrogen bonds are shown as dotted lines.

Table 1. Important Backbone Torsion Angles (deg) for Peptide 1

Aib	ϕ_1/deg	ψ_1/deg	ϕ_3/deg	ψ_3/deg
A	−57.84	−43.27	59.68	39.53
B	61.09	48.62	−54.27	−45.28
cinnamic	ϕ_2/deg	ψ_2/deg	ϕ_4/deg	ψ_4/deg
A	171.70	−176.72	−24.51	−164.37
B	−179.10	−171.19	11.66	−3.17

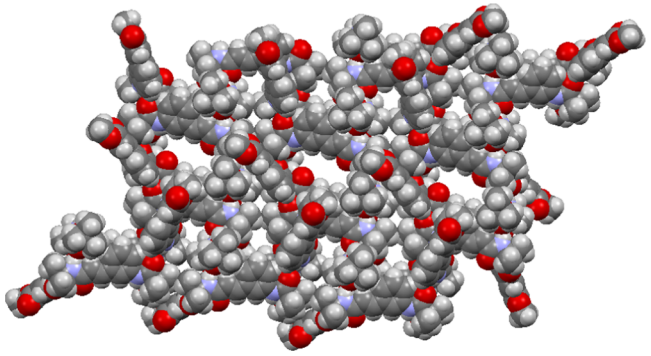

Figure 7. Higher order assembly of α,ε-hybrid peptide foldamer **1** to form porous structure.

To determine the conformational properties of the peptides in solution, NMR experiments were performed. The variable temperature ^{1}H NMR experiment of peptide **1** in $CDCl_3$ exhibits very little shifts of the amide protons with increasing temperature, indicating hydrogen-bonded stable structure in solution (Figures S1 and S2, Supporting Information). Generally, incorporation of small amounts of hydrogen bond-accepting solvents like dimethyl sulfoxide (DMSO)-d_6 in $CDCl_3$ solution of peptide results in monotonic downfield shifts of exposed NH functions, leaving solvent-shielded NH functions almost unaffected.[29] The effects of adding DMSO-d_6 to $CDCl_3$ solutions of peptide **1** are reported in Figure S3 in the Supporting Information. Figure S4 in the Supporting Information shows that Aib(1), Aib(3), and Aca(4) NHs are solvent exposed, as evident from their significant chemical shift changes ($\Delta\delta$ −0.23, 0.33, and −0.39, respectively) upon the addition of DMSO-d_6 in $CDCl_3$ solutions. Aca(2) NH exhibits

DOI: 10.1021/acsomega.8b00832
ACS Omega 2018, 3, 8760−8768

Table 2. Hydrogen Bonding Parameters of Peptide 1[a]

D−H···A	D···H (Å)	H···A (Å)	D···A (Å)	D−H···A (deg)
N00C−H00C···O00A	0.88	2.19	3.038(5)	163[a]
N00D−H00D···O007	0.88	2.17	3.026(5)	163
N00E−H00E···O001	0.88	1.97	2.822(5)	161[b]
N00F−H00F···O003	0.88	2.18	2.993(5)	154
N00F−H00F···O00D	0.88	2.42	2.788(6)	106
N00G−H00G···O002	0.88	2.09	2.940(3)	162
N00I−H00I···O00E	0.88	2.47	2.826(6)	105
N00I−H00I···O005	0.88	2.17	2.999(5)	157[b]
N00J−H00J···N006	0.88	2.27	3.125(5)	165
N00J−H00J···N00G	0.88	2.42	2.795(5)	106
N00K−H00J···N2	0.88	1.99	2.822(5)	157
N00K−H00K···N00C	0.88	2.40	2.798(5)	108

[a]Symmetry equivalent: $a = -x, 1 - y, 1 - z$; $b = 1 - x, -1/2 + y, 3/2 - z$.

very little chemical shift change ($\Delta\delta$ −0.09) for peptide **1** even at higher percentages of DMSO-d_6. Therefore, the results obtained from the solution-state studies are consistent with the peptide **1** conformation in the crystal. Table S1 in the Supporting Information shows $\Delta\delta$ values of all NHs for peptide **1**. On the other hand, temperature-dependent ^{1}H NMR experiment of the saturated peptide **2** in $CDCl_3$ also exhibits little shifts of the amide protons with increasing temperature, indicating hydrogen-bonded stable structure in solution. Whereas on the addition of DMSO-d_6 to $CDCl_3$ solutions of peptide **2** (Figure S4 in the Supporting Information), Aib(1) and Aib(3) NHs undergo significant chemical shift change ($\Delta\delta$ 0.66 and 1.24, respectively). Interestingly, AcaH(2) and AcaH(4) NHs exhibit minimal chemical shift change ($\Delta\delta$ −0.22 and −0.11, respectively) even at higher percentages of DMSO-d_6. The results suggest that peptide **2** forms intramolecular hydrogen-bonded folded structure in $CDCl_3$ solution.[29] Table S2 in the Supporting Information shows $\Delta\delta$ values of all NHs for peptide **2**.

Considering the porous structure of α,ε-hybrid peptide foldamer **1**, a wide range of organic solvents were tested to make gel by using the traditional heating−cooling technique and other methods.[23] But the unsaturated tetrapeptide **1** did not form gel. On the other hand, the saturated peptide **2** was found to form gel (Figure 8) in most of the aromatic solvents like xylene, toluene, 1,2-dichlorobenzene, etc. The phase-selective gelation was confirmed by the inverted vial experiment (Figure 8).[23] The transparent gel shows stability for 2−3 months at room temperature.

The morphology of the α,ε-hybrid peptides was examined by field emission scanning electron microscopic (FE-SEM) measurements. For FE-SEM experiments, dilute solutions (0.5 mM) of corresponding peptides were drop casted on microscopic glass slides and finally dried under vacuum for 2 days. Figure 9 depicts the FE-SEM images of the peptides **1** and **2**. From Figure 9a,b, the peptide **1** shows the polydisperse microspheres morphology. The average diameter of the microspheres is ca. 1 μm. From Figure 9c,d, the peptide **2** xerogel from xylene exhibits ribbons-like morphology. The diameter of the ribbons is ca. 500 nm and several micrometers in length.

The macroscopic character of the gel was obtained primarily from the rheology measurement.[24] Both G', a parameter for the elastic response of the gel (the storage modulus), and G'', a measure of the viscous response (the loss modulus), were examined at 25 °C as a function of time. For organogel (10 mg/mL) of peptide **2**, the storage modulus (G') was found to be approximately an order of magnitude higher than the loss modulus (G''), suggesting an elastic rather than a viscous sample (Figure 10). Such a rheological response is a characteristic, mainly shown by gel networks that have physical cross-links through weak co-operative interactions.[24]

Presently, water pollution by organic dyes is a major problem for the global community. Most of these dyes are discharged from textile, cosmetic, and other industries. Even very low concentrations of dyes in the waste water are undesirable as well as toxic for living cells.[25] Most of these dyes are nondegradable due to their robust chemical structures.[26] In this context, gels can be used to purify water from dyes.[27,28] For this purpose, 1 mM solution of dyes rhodamine 6G (cationic), methyl violet (cationic), methyl orange (anionic), and pyrocatechol violet (neutral) was prepared. Then, 2 mL of these solutions were placed in vials containing gel of α,ε-hybrid peptide **2** in xylene. The peptide **2** gel was found to absorb the cationic dyes selectively. The reason behind the absorption of only cationic dyes may be attributed to the presence of aromatic rings and the amide bonds that make the peptide neutral but electron rich. This electron-rich peptide can easily undergo attractive interactions with the cationic dyes but not with anionic or neutral dyes due to repulsive interactions. The absorption of dyes was very rapid, and this was studied by UV/vis spectroscopy (Figure 11). Within 24 h, more than 95% removal of the dyes was observed. The gel can also absorb a mixture of cationic dyes (rhodamine and methyl violet) selectively from waste water (a mixture of dyes, including cationic, anionic, and neutral dyes). The results obtained have been included in the Figure S5 Supporting Information. The

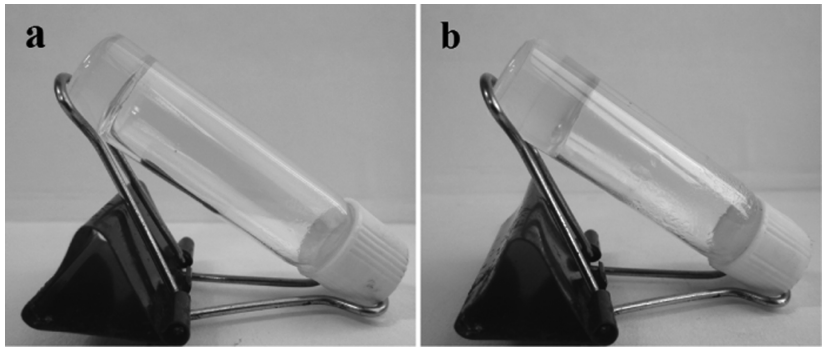

Figure 8. (a) Inverted vial confirms the gelation of peptide **2** in xylene; (b) the phase-selective gelation of peptide **2** from xylene−water mixture.

DOI: 10.1021/acsomega.8b00832
ACS Omega 2018, 3, 8760−8768

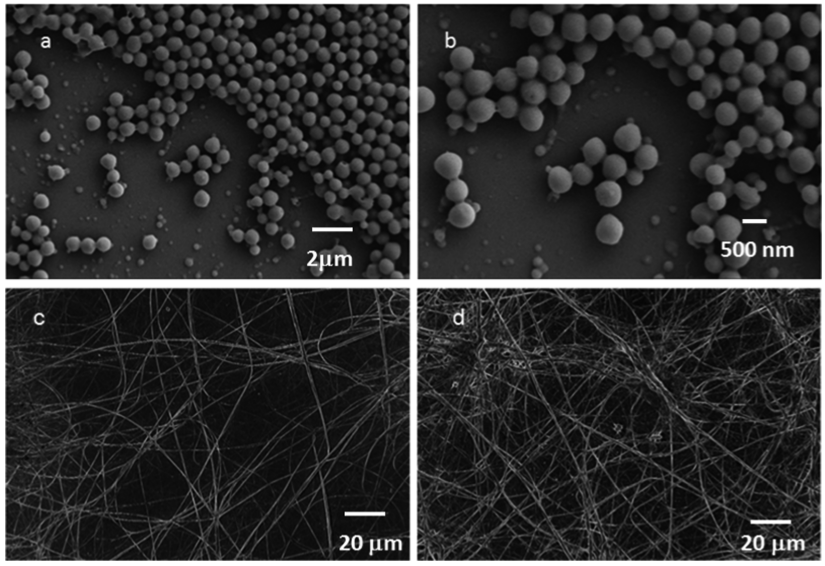

Figure 9. (a, b) FE-SEM images of unsaturated α,ε-hybrid peptide **1** showing polydisperse microspheres morphology. (c, d) FE-SEM images of the xerogel of saturated α,ε-hybrid peptide **2** from *p*-xylene showing ribbons-like entangled network.

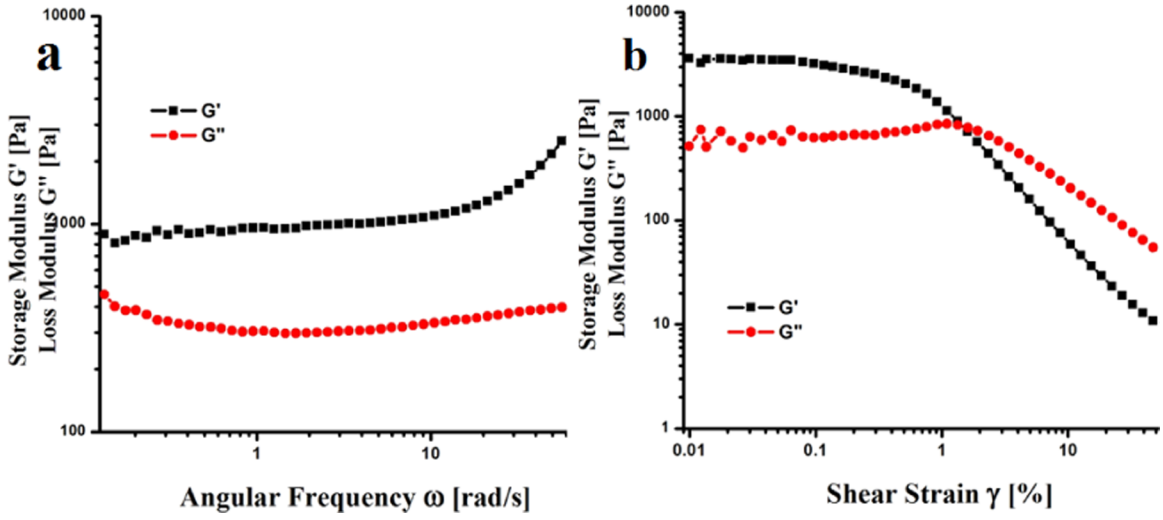

Figure 10. Rheology data of peptide **2** gel in xylene at 25 °C (10 mg/mL); (a) frequency sweep of the gel at a strain of 0.1%; (b) strain sweep of the gel at a frequency of 1 rad/s.

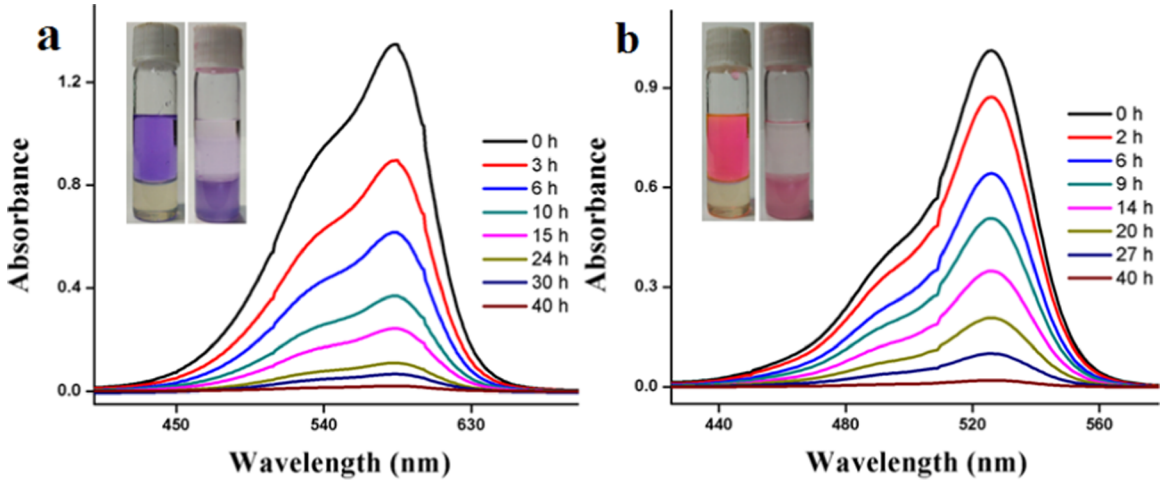

Figure 11. Dye removal studies using peptide **2** gel in xylene; (a) methyl violet and (b) rhodamine 6G.

DOI: 10.1021/acsomega.8b00832
ACS Omega 2018, 3, 8760−8768

peptide **2** gel can be reused several times for the cationic dye removal. For this purpose, first, we let the gel absorb the dyes (cationic) and then the gel−dye mixture was treated with deionized water.[30] The mixture undergoes removal of the dyes.[31] The process was repeated three times, and the removal (visually) of dyes occurred in each case.

CONCLUSIONS

In conclusion, we have discussed the effect of geometrically rigid trans α,β-unsaturated ε-amino acids on the conformation and assembly of α,ε-hybrid peptide foldamers. The unsaturated α,ε-hybrid peptide foldamer **1** has stapler-pin-like structure in solid state. Two molecules of α,ε-hybrid peptide foldamer **1** in the asymmetric unit are stabilized by multiple intermolecular hydrogen bonding interactions and $\pi-\pi$ stacking interactions. Unsaturated α,ε-hybrid peptide foldamer **1** does not form organogel. But on hydrogenation, saturated α,ε-hybrid peptide foldamer **2** forms instant gel in most of the aromatic solvents. The gel exhibits high stability and can be used to remove cationic organic pollutants from waste water efficiently. These α,ε-hybrid peptide foldamers containing functionalizable carbon−carbon double bonds in peptide backbone may provide advanced functional materials by postsynthetic modification.

EXPERIMENTAL SECTION

General. All reagents were procured from SRL. *m*-Nitrobenzaldehyde and malonic acid were bought from Sigma chemicals.

Peptide Synthesis. The peptide **1** was synthesized by the traditional solution phase method.[32] The amino acid C-terminus was protected by methyl ester formation. Coupling was promoted by dicyclohexylcarbodiimide (DCC). The peptide **2** was synthesized by hydrogenation of peptide **1** using hydrogen and Pd/C. The purification of products was done using column chromatography on silica gel (mesh size 100−200), with *n*-hexane−ethyl acetate solution as eluent. The reaction intermediates and final peptides were fully characterized by ^{1}H NMR (400 and 500 MHz) spectroscopy, ^{13}C NMR (125 MHz) spectroscopy, mass spectrometry, and FT-IR spectroscopy analysis. Further, X-ray crystallography was performed to characterize the peptide **1**.

trans-3-Nitrocinnamic Acid ***4***. A mixture of *m*-nitrobenzaldehyde (4.53 g, 30 mmol), malonic acid (5.2 g, 50 mmol), piperidine (0.4 mL, 4 mmol), and dimethylformamide−water (46 mL, 20:3) was heated at 120 °C for 6 h, cooled, and poured into water (100 mL). The mixture was filtered, and the residue was washed by water (3 × 20 mL) and recrystallized from methanol. The crystals were taken in ethyl acetate and neutralized with a dilute solution of $KHSO_4$. The ethyl acetate extract was dried by using anhydrous sodium sulfate and concentrated in vacuum.[33] The pure compound was obtained as a yellow solid. Yield: 4.25 g (22 mmol, 73.34%). ^{1}H NMR (400 MHz, DMSO-d_6, δ ppm): 12.62 [1H, bs, COOH], 8.52−8.53 [1H, t, ArH], 8.22−8.25 [1H, m, ArH], 8.18−8.19 [1H, d, vinylic CH], 7.69−7.75 [2H, m, ArH], 6.73−6.77 [1H, d, vinylic CH]. ^{13}C NMR (125 MHz, DMSO-d_6, δ ppm): 167.07, 148.31, 141.42, 136.1, 133.97, 130.31, 124.32, 122.75, 122.28.

Methyl (E)-3-Nitrocinnamate ***5***. A solution of **4** (1.93 g, 10 mmol) in methanol (50 mL) was stirred and cooled in an ice-water bath. Thionyl chloride (2.5 mL, 34.46 mmol) was added drop wise and stirred continuously at room temperature for 6 h. Addition of water (100 mL) liberated the product, which was extracted with ethyl acetate and the ethyl acetate layer was washed with water (3 × 50 mL). The extract was then dried by using anhydrous sodium sulfate and concentrated under vacuum.[33] The pure product was obtained as a yellow crystalline solid. Yield: 1.99 g (9.61 mmol, 96.1%). ^{1}H NMR (500 MHz, DMSO-d_6, δ ppm): 8.55 [1H, s, ArH], 8.23−8.25 [1H, m, ArH], 8.19−8.2 [1H, d, J = 7.88, ArH], 7.78−7.81 [1H, d, J = 16.08, vinylic CH], 7.69−7.72 [1H, m, ArH], 6.84−6.87 [1H, d, J = 16.08, vinylic CH], 3.75 [3H, s, OCH_3]. ^{13}C NMR (125 MHz, DMSO-d_6, δ ppm): 166.31, 148.35, 142.13, 135.9, 134.08, 130.32, 124.55, 122.97, 120.79, 51.7.

Methyl (E)-3-Aminocinnamate ***6***. A mixture of **5** (1.04 g, 5 mmol), water (5 mL), acetic acid (20 mL), and Fe dust (15 g) in acetone (80 mL) was heated at 100 °C for 3 h and cooled; then, the solution was filtered through silica bed (230−400 mesh) and the filtrate was evaporated and diluted with water (50 mL). The aqueous layer was extracted by ethyl acetate (3 × 50 mL), and the extract was washed with 1 M sodium carbonate (3 × 50 mL) and brine (2 × 50 mL). The extract was dried by using anhydrous sodium sulfate and concentrated under vacuum to get the compound **6** as a pure product. Yield: 0.84 g, (4.74 mmol, 94.81%). ^{1}H NMR (500 MHz, $CDCl_3$, δ ppm): 7.58−7.62 [1H, d, J = 16.02, vinylic CH], 7.15−7.18 [1H, m, ArH], 6.91−6.93 [1H, d, J = 7.63, ArH], 6.82 [1H, bs, ArH], 6.69−6.71 [1H, m, ArH], 6.36−6.39 [1H, d, J = 16.02, vinylic CH], 3.79 [3H, s, OCH_3], 3.69−3.76 [2H, b, NH_2]. ^{13}C NMR (125 MHz, $CDCl_3$, δ ppm): 167.66, 146.95, 145.35, 135.58, 129.91, 118.82, 117.8, 117.26, 114.28, 51.77.

Boc-Aib-OH ***7***. 2-Aminoisobutyric acid (5.2 g, 50 mmol), 1,4-dioxane (80 mL), water (30 mL), and 2 M NaOH (50 mL) were mixed and cooled in an ice-water bath. Di-*tert*-butylpyrocarbonate (13.8 mL, 60 mmol) was mixed and stirred continuously at room temperature for 6 h. Finally, the mixture was concentrated (50−60 mL) under vacuum, cooled in an ice-water bath, covered with 60 mL of ethyl acetate, and acidified using dilute solution of $KHSO_4$, adjusting to pH 2−3. The aqueous solution was treated with ethyl acetate, and this process was repeated 2−4 times. The ethyl acetate layers were pooled, washed with water, and dried by using anhydrous sodium sulfate and concentrated in vacuum.[33] The pure compound was obtained as a white solid. Yield: 9.04 g (44.48 mmol, 88.96%). ^{1}H NMR (500 MHz, DMSO-d_6, δ ppm): 12.13 [1H, bs, COOH], 6.97 [1H, bs, NH], 1.36 [9H, s, BOC], 1.29 [6H, s, Aib C$^\beta$H]. ^{13}C NMR (125 MHz, DMSO-d_6, δ ppm): 176.16, 154.52, 77.62, 54.96, 28.18, 25.12.

Boc-Aib-Aca-OMe ***8***. Boc-Aib-OH (1.62 g, 8 mmol) was dissolved in 25 mL of dry DCM in an ice-water bath. Compound **6** (0.71 g, 4 mmol) was added to the solution, followed immediately by DCC (1.65 g, 8 mmol). The solution was cooled to room temperature and stirred for 48 h. DCM was evaporated, and the solid was mixed with ethyl acetate (50 mL), and dicyclohexylurea (DCU) was separated by filtration. The organic layer was cleaned with 2 M HCl (3 × 30 mL), brine (2 × 30 mL), and 1 M sodium carbonate (3 × 30 mL) and dried by using anhydrous sodium sulfate and concentrated in vacuum. The compound was purified by silica gel (100−200 mesh) using *n*-hexane−ethyl acetate (4:1) as eluent to yield peptide **8** as a white solid. Yield: 0.84 g (2.32 mmol, 58%). ^{1}H NMR (400 MHz, $CDCl_3$, δ ppm): 7.79 [1H, m, ArH], 7.63−7.67 [1H, d, J = 16.02, vinylic CH], 7.48−7.5 [1H, m, ArH], 7.3−7.34 [1H, m, ArH], 7.23−7.25 [1H, d, J = 7.63, ArH],

DOI: 10.1021/acsomega.8b00832
ACS Omega 2018, 3, 8760−8768

6.42−6.46 [1H, d, J = 16.02, vinylic CH], 4.94 [1H, bs, Ar NH], 3.79 [3H, s, OCH_3], 1.7 [1H, s, Aib NH], 1.57 [6H, s, Aib $C^{\beta}H$], 1.44 [9H, s, BOC]. ^{13}C NMR (125 MHz, $CDCl_3$, δ ppm): 172.94, 166.44, 155.91, 144.7, 135.37, 129.57, 123.95, 122.88, 121.65, 119.21, 118.51, 81.28, 58.06, 51.76, 28.41, 25.82.

Boc-Aib-Aca-OH ***9***. To 0.36 g (1 mmol) of compound **8**, 10 mL of methanol and 4 mL of 2 M sodium hydroxide solution were added[34] and stirred and the saponification reaction was monitored by thin layer chromatography (TLC). After 10 h, MeOH was dried under vacuum; the residue was mixed with 30 mL of water and treated with diethyl ether (2 × 30 mL). Finally, the pH of the aqueous layer was fixed at 2−3 using 1 M HCl and it was treated with ethyl acetate (3 × 30 mL). The extracts were pooled, dried by using anhydrous sodium sulfate, and concentrated under vacuum to obtain compound **9** as a white solid. Yield 0.29 g (0.83 mmol, 83%).

H_2N-Aib-Aca-OMe ***10***. To 0.36 g (1 mmol) of compound **8**, 5 mL of trifluoroacetic acid (TFA) was added and deprotection of BOC group was examined by TLC. After 6 h, TFA was removed under reduced pressure and the residue was neutralized by Et_3N.

Boc-Aib-Aca-Aib-Aca-OMe ***1***. Compound **9** (0.29 g, 0.83 mmol) was mixed in 20 mL of dry DCM in an ice-water bath. Compound **10** was then added to the solution, followed immediately by 0.21 g (1 mmol) of DCC. The reaction was cooled to room temperature and stirred for 48 h. DCM was dried, and the product was mixed with ethyl acetate (40 mL), and dicyclohexylurea (DCU) was filtered off. The organic layer was treated with 2 M HCl (3 × 30 mL), brine (2 × 30 mL), and 1 M sodium carbonate (3 × 30 mL). The extract was then dried by using anhydrous sodium sulfate and concentrated under vacuum. The product was purified by silica gel (100−200 mesh) using n-hexane−ethyl acetate (3:1) as eluent to yield peptide **1** as a white solid. Yield: 0.24 g (0.4 mmol, 48.19%). ^1H NMR (400 MHz, DMSO-d_6, δ ppm): 9.52 [2H, s, Ar NH], 8.4 [1H, s, Aib NH], 8.07 [1H, bs, Aib NH], 7.91 [1H, b, ArH], 7.69−7.72 [1H, m, ArH], 7.57−7.61 [1H, d, J = 16.02, vinylic CH], 7.46 [1H, b, ArH], 7.29−7.39 [4H, m, ArH], 7.18−7.2 [1H, d, J = 7.92, vinylic CH], 6.92−7.02 [1H, m, ArH], 6.71−6.75 [1H, d, J = 15.26, vinylic CH], 6.48−6.52 [1H, d, J = 16.02, vinylic CH], 3.72 [3H, s, OCH_3], 1.48 [6H, s, Aib $C^{\beta}H$], 1.38 [9H, s, BOC], 1.22−1.25 [6H, m, Aib $C^{\beta}H$]. ^{13}C NMR (125 MHz, DMSO-d_6, δ ppm): 173, 166.5, 164.49, 144.51, 139.91, 138.81, 135.02, 134.04, 128.91, 123.21, 122.77, 122.5, 122.08, 121.01, 119.26, 117.75, 78.19, 56.57, 51.49, 28.19, 25.04.

Boc-Aib-AcaH-Aib-AcaH-OMe ***2***. To the suspension of **1** (0.12 g, 0.2 mmol) in 10 mL of ethyl acetate, 50 mg of Pd/C (10%) was added and stirred vigorously for 8 h under hydrogen atmosphere. Progress of the reduction reaction was examined by TLC. After completion of the reaction, 50 mL of ethyl acetate was added into it and the solution was filtered through a silica bed and the filtrate was dried under vacuum to yield 0.115 g (0.193 mmol, 96.5%) of the pure peptide **2** as a white solid. ^1H NMR (500 MHz, $CDCl_3$, δ ppm): 9.25 [1H, s, Ar NH], 8.89 [1H, b, Ar NH], 7.63 [1H, b, ArH], 7.35 [1H, b, ArH], 7.27−7.29 [1H, m, ArH], 7.16−7.2 [1H, m, ArH], 7.09−7.1 [2H, m, ArH], 6.89−6.9 [2H, d, J = 6.48 ArH], 6.09 [1H, bs, Aib NH], 4.98 [1H, s, Aib NH], 3.66 [3H, s, OCH_3], 2.88−2.91 [4H, m, $2CH_2$], 2.59−2.62 [2H, t, CH_2], 2.48−2.51 [2H, t, CH_2], 1.54 [6H, s, Aib $C^{\beta}H$], 1.52 [6H, s, Aib $C^{\beta}H$], 1.43 [9H, s, BOC]. ^{13}C NMR (125 MHz, $CDCl_3$, δ ppm): 173.49, 173.21, 172.34, 155.42, 141.42, 138.64, 138.51, 129.19, 129.05, 124.67, 124.02, 120.17, 119.76, 118.36, 117.99, 81.07, 58.8, 57.78, 51.74, 38.38, 35.78, 31.49, 31.05, 29.82, 28.4, 25.78, 25.45.

NMR Experiments. All NMR spectroscopy were done on a 400 MHz Jeol or 500 MHz Bruker spectrometer. Compound concentrations were in the 1−10 mM range in DMSO-d_6 and $CDCl_3$ solution.[31]

FT-IR Experiments. FT-IR spectroscopy in the solid state was performed with a Perkin Elmer Spectrum RX1 spectrophotometer using KBr disk method.

Absorption Spectroscopy. The absorption spectra of peptides were measured on a Perkin Elmer UV/vis spectrometer (Lambda 35) using a quartz cell having 1 cm path length.

Fluorescence Spectroscopy. The fluorescence spectra have been recorded on a Perkin Elmer fluorescent spectrometer (LS 55) using a quartz cell having 1 cm path length. Slits of 2.5/2.5 width were used.

Mass Spectrometry. Mass spectrometry was carried out on a Waters Corporation Q-Tof Micro YA263 high-resolution mass spectrometer by electrospray ionization (positive mode).

Field Emission Scanning Electron Microscopy. Field emission scanning electron microscopy (FE-SEM) was performed to examine the morphologies of the synthesized peptides. A drop of peptide solution was casted on a clean microscopic glass slide and dried under vacuum. The samples were gold-coated, and the images were captured in an FE-SEM apparatus (Jeol Scanning Microscope-JSM-6700F).

Gelation. The peptide **2** (5 mg) was mixed in 1 mL of solvent, and gel was obtained by heating−cooling technique.

Rheology Experiments. To examine the thixotropic behavior and mechanical strength of the gel, we have done rheological measurements on a MCR 102 rheometer (Anton Paar, Modular Compact Rheometer) by a steel parallel plate geometry having 40 mm diameter at 20 °C. The rheometer was attached to a Peltier circulator thermocube to control the temperature accurately. The storage modulus (G') and loss modulus (G'') of the gel were then recorded by using the setup.[31]

X-ray Crystallography. Diffraction quality light yellow color crystals of peptide **1** were obtained from methanol−water solution by slow evaporation. Intensity data were collected with Mo Kα radiation by a Bruker APEX-2 CCD diffractometer. Data were processed using Bruker SAINT package. The structure solution and refinement were performed by SHELX97. Refinement of nonhydrogen atoms was performed using anisotropic thermal parameters.[31] Crystal data of compound **1**: $C_{32}H_{40}N_4O_7$, M_w = 592.68, $P12_1/c1$, a = 21.5402(19) Å, b = 17.4732(14) Å, c = 19.4743(15) Å, α = 90°, β = 114.956(3)°, γ = 90°, V = 6645.3(10) Å^3, Z = 8, d_m = 1.185 Mg/m^3, K = 100, R_1 = 0.0812, and wR_2 = 0.1873 for 9841 data with $I > 2\sigma(I)$. CCDC 1505412 contains the crystallographic data for peptide **1**. The data was submitted at the Cambridge Crystallographic Data Centre with CCDC reference 1834467.

■ ASSOCIATED CONTENT

Ⓢ Supporting Information

The Supporting Information is available free of charge on the ACS Publications website at DOI: 10.1021/acsomega.8b00832.

DOI: 10.1021/acsomega.8b00832
ACS Omega 2018, 3, 8760−8768

Synthesis and characterizations of peptides, ^{1}H NMR, ^{13}C NMR, and Figures S1−S17 (PDF)

AUTHOR INFORMATION

Corresponding Author

*E-mail: deba_h76@yahoo.com, deba_h76@iiserkol.ac.in.

ORCID

Debasish Haldar: 0000-0002-7983-4272

Author Contributions

M.D. has synthesized the compounds. M.D., T.D., and D.P. have performed the experimental works. D.H. has done the analysis and written the manuscript.

Notes

The authors declare no competing financial interest.

ACKNOWLEDGMENTS

We acknowledge the CSIR, India for financial assistance (Project No. 02(0206)/14/EMR-II). This work is also supported by CSIR, India (fellowship to M.D., T.D., and D.P.).

REFERENCES

(1) Hecht, S.; Huc, I. *Foldamers: Structure, Properties, and Applications*; Wiley-VCH: Weinheim, 2007.

(2) Gellman, S. H. Foldamers: A Manifesto. *Acc. Chem. Res.* **1998**, *31*, 173−180.

(3) Hill, D. J.; Mio, M. J.; Prince, R. B.; Hughes, T. S.; Moore, J. S. A Field Guide to Foldamers. *Chem. Rev.* **2001**, *101*, 3893−4012.

(4) Karle, I. L.; Pramanik, A.; Banerjee, A.; Bhattacharya, S.; Balaram, P. ω-Amino Acids in Peptide Design. Crystal Structures and Solution Conformations of Peptide Helices Containing a β-Alanyl-γ-Aminobutyryl Segment. *J. Am. Chem. Soc.* **1997**, *119*, 9087−9095.

(5) Roy, R. S.; Gopi, H. N.; Raghothama, S.; Karle, I. L.; Balaram, P. Hybrid Peptide Hairpins Containing α- and ω-Amino Acids: Conformational Analysis of Decapeptides with Unsubstituted β-, γ-, and δ-Residues at Positions 3 and 8. *Chem. - Eur. J.* **2006**, *12*, 3295−3302.

(6) Rai, R.; Vasudev, P. J.; Ananda, K.; Raghothama, S.; Shamala, N.; Karle, I. L.; Balaram, P. Hybrid Peptides: Expanding the β Turn in Peptide Hairpins by the Insertion of β-, γ-, and δ-Residues. *Chem. - Eur. J.* **2007**, *13*, 5917−5926.

(7) Daniels, D. S.; Petersson, E. J.; Qiu, J. X.; Schepartz, A. High-Resolution Structure of a β-Peptide Bundle. *J. Am. Chem. Soc.* **2007**, *129*, 1532−1533.

(8) Petersson, E. J.; Schepartz, A. Toward β-Amino Acid Proteins: Design, Synthesis, and Characterization of a Fifteen Kilodalton β-Peptide Tetramer. *J. Am. Chem. Soc.* **2008**, *130*, 821−823.

(9) Lee, B. C.; Zuckermann, R. N.; Dill, K. A. Folding a Nonbiological Polymer into a Compact Multihelical Structure. *J. Am. Chem. Soc.* **2005**, *127*, 10999−11009.

(10) Delsuc, N.; Leger, J. M.; Massip, S.; Huc, I. Proteomorphous Objects from Abiotic Backbones. *Angew. Chem.* **2007**, *119*, 218−221.

(11) Haldar, D.; Schmuck, C. Metal-free double helices from abiotic backbones. *Chem. Soc. Rev.* **2009**, *38*, 363−371.

(12) Aravinda, S.; Shamala, N.; Balaram, P. Aib Residues in Peptaibiotics and Synthetic Sequences: Analysis of Nonhelical Conformations. *Chem. Biodiversity* **2008**, *5*, 1238−1262.

(13) Venkatraman, J.; Shankaramma, S. C.; Balaram, P. Design of Folded Peptides. *Chem. Rev.* **2001**, *101*, 3131−3152.

(14) Choi, S. H.; Guzei, I. A.; Spencer, L. C.; Gellman, S. H. Crystallographic Characterization of Helical Secondary Structures in α/β-Peptides with 1:1 Residue Alternation. *J. Am. Chem. Soc.* **2008**, *130*, 6544−6550.

(15) Guo, L.; Chi, Y.; Almeida, A. M.; Guzei, I. A.; Parker, B. K.; Gellman, S. H. Stereospecific Synthesis of Conformationally Constrained γ-Amino Acids: New Foldamer Building Blocks That Support Helical Secondary Structure. *J. Am. Chem. Soc.* **2009**, *131*, 16018−16020.

(16) Guo, L.; Almeida, A. M.; Zhang, W.; Reidenbach, A. G.; Choi, S. H.; Guzei, I. A.; Gellman, S. H. Helix Formation in Preorganized β/γ-Peptide Foldamers: Hydrogen-Bond Analogy to the α-Helix without α-Amino Acid Residues. *J. Am. Chem. Soc.* **2010**, *132*, 7868−7869.

(17) Kumar, M. G.; Thombare, V. J.; Katariya, M. M.; Veeresh, K.; Raja, K. M. P.; Gopi, H. N. Non-classical helices with cis carbon-carbon double bonds in the backbone: structural features of α,γ-hybrid peptide foldamers. *Angew. Chem., Int. Ed.* **2016**, *55*, 7847−7851.

(18) Misra, R.; Dey, S.; Reja, R. M.; Gopi, H. N. Artificial β-Double Helices from Achiral γ-Peptides. *Angew. Chem., Int. Ed.* **2018**, *57*, 1057−1061.

(19) Cain, B. F.; Atwell, G. J.; Denny, W. A. Potential antitumor agents. 23. 4′-(9-Acridinylamino)alkanesulfonanilide congeners bearing hydrophilic functionality. *J. Med. Chem.* **1977**, *20*, 987−996.

(20) Galan, B. R.; Reback, M. L.; Jain, A.; Appel, A. M.; Shaw, W. J. Electrocatalytic Oxidation of Formate with Nickel Diphosphine Dipeptide Complexes: Effect of Ligands Modified with Amino Acids. *Eur. J. Inorg. Chem.* **2013**, *2013*, 5366−5371.

(21) Moretto, V.; Crisma, M.; Bonora, G. M.; Toniolo, C.; Balaram, H.; Balaram, P. Comparison of the effect of five guest residues on the .beta.-sheet conformation of host (L-val)n oligopeptides. *Macromolecules* **1989**, *22*, 2939−2944.

(22) Banerjee, A.; Maji, S. K.; Drew, M. G. B.; Haldar, D.; Banerjee, A. Amyloid-like fibril-forming supramolecular β-sheets from a β-turn forming tripeptide containing non-coded amino acids: the crystallographic signature. *Tetrahedron Lett.* **2003**, *44*, 335−339.

(23) Maity, S.; Jana, P.; Haldar, D. Fabrication of nanoporous material from a hydrophobic peptide. *CrystEngComm* **2011**, *13*, 3064−3071.

(24) Baral, A.; Roy, S.; Dehsorkhi, A.; Hamley, I. W.; Mohapatra, S.; Ghosh, S.; Banerjee, A. Assembly of an Injectable Noncytotoxic Peptide-Based Hydrogelator for Sustained Release of Drugs. *Langmuir* **2014**, *30*, 929−936.

(25) de Luna, L. A. V.; da Silva, T. H. G.; Nogueira, R. F. P.; Kummrow, F.; Umbuzeiro, G. A. Aquatic toxicity of dyes before and after photo-Fenton treatment. *J. Hazard. Mater.* **2014**, *276*, 332−338.

(26) Robinson, T.; McMullan, G.; Marchant, R.; Nigam, P. Remediation of dyes in textile effluent: a critical review on current treatment technologies with a proposed alternative. *Bioresour. Technol.* **2001**, *77*, 247−255.

(27) Okesola, B. O.; Smith, D. K. Applying low-molecular weight supramolecular gelators in an environmental setting−selfassembled gels as smart materials for pollutant removal. *Chem. Soc. Rev.* **2016**, *45*, 4226−4251.

(28) Basak, S.; Nandi, N.; Paul, S.; Hamley, I. W.; Banerjee, A. A tripeptide-based self-shrinking hydrogel for waste-water treatment: removal of toxic organic dyes and lead (Pb2+) ions. *Chem. Commun.* **2017**, *53*, 5910−5913.

(29) Maji, S. K.; Banerjee, R.; Velmurugan, D.; Razak, A.; Fun, H. K.; Banerjee, A. Peptide Design Using ω-Amino Acids: Unusual Turn Structures Nucleated by an N-Terminal Single γ-Aminobutyric Acid Residue in Short Model Peptides. *J. Org. Chem.* **2002**, *67*, 633−639.

(30) Cheng, N.; Hu, Q.; Guo, Y.; Wang, Y.; Yu, L. Efficient and Selective Removal of Dyes Using Imidazolium-Based Supramolecular Gels. *ACS Appl. Mater. Interfaces* **2015**, *7*, 10258−10265.

(31) Nandi, S. K.; Maji, K.; Haldar, D. Self-healing hydrogel from a dipeptide and HCl sensing. *ACS Omega* **2018**, *3*, 3744−3751.

(32) Sarkar, R.; Debnath, M.; Maji, K.; Haldar, D. Solvent assisted structural diversity: supramolecular sheet and double helix of a short aromatic γ-peptide. *RSC Adv.* **2015**, *5*, 76257−76262.

(33) Maity, S.; Jana, P.; Maity, S. K.; Haldar, D. Fabrication of Hollow Self-Assembled Peptide Microvesicles and Transition from Sphere-to-Rod Structure. *Langmuir* **2011**, *27*, 3835−3841.

(34) Ray, S.; Takafuji, M.; Ihara, H. Amino-acid-based, lipid-directed, in situ synthesis and fabrication of gold nanoparticles on

DOI: 10.1021/acsomega.8b00832
ACS Omega 2018, 3, 8760−8768

silica: a metamaterial framework with pronounced catalytic activity. *Nanotechnology* **2012**, *23*, No. 495301.

DOI: 10.1021/acsomega.8b00832
ACS Omega 2018, 3, 8760−8768